Adsorption (2015) 21:67–75
DOI 10.1007/s10450-015-9650-3

Experimental and numerical study on water sorption over modified mesoporous silica

Hongyin Chen · Weilong Wang · Xiaolan Wei · Jing Ding · Jianping Yang

Received: 8 July 2014 / Revised: 11 October 2014 / Accepted: 12 January 2015 / Published online: 21 January 2015

Abstract $-SO_3H$ modified mesoporous silica adsorbent with water sorption capacity and fast desorption kinetics for water sorption was synthesized and studied via a combined experimental and numerical approach. Mesoporous silica was synthesized using sol–gel method in H_2SO_4 medium. The water adsorption isotherms and kinetics over the silica were evaluated by a dynamic water vapor sorption analyzer. Mesoporous silica was modeled using annealing simulation with CVFF forcefield. $-SO_3H$ modified mesoporous silica was modeled by the attachment of $-SO_3H$ to the surface hydroxyl groups and validated. Simulation results show water sorption capacity at low relative humidity (RH) increases with $-SO_3H$ loading on mesoporous silica. Energy distribution of intermolecular interaction and micro-view of water sorption over $-SO_3H$ modified mesoporous silica reveal that although strong interaction (intermolecular interaction of −40 to −20 kcal/mol) between hydrophilic groups ($-SO_3H$) with water can increase water sorption capacity at low RH, weak H_2O–H_2O interaction (intermolecular interaction of −20 to −10 kcal/mol) dominated water sorption capacity at both low and high RH.

Electronic supplementary material The online version of this article (doi:10.1007/s10450-015-9650-3) contains supplementary material, which is available to authorized users.

H. Chen · W. Wang (✉) · J. Ding
Center for Energy Conservation Technology, School of Engineering, Sun Yat-sen University, Guangzhou, China
e-mail: wwlong@mail.sysu.edu.cn

X. Wei · J. Yang
School of Chemistry and Chemical Engineering, South China University of Technology, Guangzhou, China

Keywords Molecular simulation · Mesoporous silica · Sulfonic modification · Water vapor sorption

1 Introduction

Adsorption on porous solid materials is a promising technology for dehumidification with low energy consumption and high efficiency (Roque-Malherbe 2007), where the adsorbent is the key. Design adsorbent with high adsorption capacity and fast kinetics for water sorption is critical considering industrial applications, i.e. rotary desiccant wheel.

Periodic mesoporous silica material has been widely used as an adsorbent due to its uniform porosity, large surface area and controllable pore size. Considering water sorption, Kocherbitov and Alfredsson (2007) studied the water sorption over MCM-41 by sorption calorimetry. Mancinelli et al. (2009) investigated the structure of water confined in MCM-41 by multi scale approach. Li et al. (2007) studied the effect of pore size on desorption activation energy experimentally. Results show that water sorption capacity over silica was determined by the density of surface hydroxyl groups at low RH. Functionalization of mesoporous silica is an effective way to change its surface property and thus affect its water sorption performance. Several routes for the modification of are described in the literature. Grafting of functional organic groups using surface hydroxyl groups as anchor points has been widely employed for different applications. Schumacher et al. (2006) and Wang et al. (2013, 2014) discussed the separation of CO_2 using organic (triethylchlorosilane, octadecyldimethylchlorosilane et al.) functionalized mesoporous silica. Ho et al. (2011) studied CO_2 sorption over functionalized MCM-41 by combined molecular simulation and

experiments. However, less work concerned functionalized mesoporous silica for water sorption.

Herein, we report a combined experimental and numerical study of a series of $–SO_3H$ modified mesoporous silica. The effects of surface sulfonate density and energy distribution of intermolecular interaction on water sorption characters were studied. Mesoporous silica was synthesized by a sol–gel way in H_2SO_4 solution and simulation structure was obtained by molecular dynamic simulation. The water adsorption isotherms and kinetics over the silica were evaluated by a dynamic water vapor sorption analyzer. Effects of surface sulfonate density on water sorption and energy distribution of intermolecular interaction were studied by molecular simulation. By combination of experimental and computational study, we can get a micro view of water vapor adsorption on the modified mesoporous silica and reveal the development of adsorption mechanism.

2 Experimental section

2.1 Synthesis method

Sol–gel process is widely applied to produce silica, glass, and ceramic materials due to its ability to form pure and homogenous products at mild conditions. Sulfonic acid-modified mesoporous silica is synthesized by means of sol–gel method in H_2SO_4 medium utilizing the following procedure. Certain amount of polyvinyl pyrrolidone (PVP, K30, average molecular weight: 58 kDa) is dissolved in distilled water and stirred for 30 min. Concentrated sulfuric acid is added by titration to keep the PH value of the solution below 1 and then stir for 30 min. Tetraethyl orthosilicate (TEOS) is added drop by drop to make sure the mole ratio of PVP:TEOS:H_2O is 1:551:26,851. The mixture solution is hydrolyzed by stirring at 328 K for 20 h and then gelled at 353 K for 48 h. Finally the gel is calcined at 773 K for 3 h with a heating rate of 0.5 K/min. Different samples named S–SiO_2–A, S–SiO_2–B, S–SiO_2–C, S–SiO_2–D are prepared by altering the hydrolysis temperature from 328 to 308 K and changing the gelation time form 48 to 24 h. S–SiO_2–A and S–SiO_2–B are hydrated under 328 K with gelation time of 48 and 24 h respectively. S–SiO_2–C and S–SiO_2–D are hydrated under 308 K with gelation time of 48 and 24 h respectively. Products are washed by distilled water to remove the free acid and then dried at 373 K overnight.

2.2 Material characterization

Specific surface area and pore radius are characterized by low temperature N_2 adsorption at 77 K using a Micromeritics Geminiv 2380 system. Prior to the measurements, samples are dried under reduced pressure at 393 K for 24 h. The surface area (S_{BET}) is determined using the BET (Brunauer–Emmett–Teller) equation over the range $P/P_0 = 0.06–0.35$. The classical pore size model developed by Barret–Joyner–Halenda (BJH) is used for the calculation for the pore volume (V_{BJH}) and pore average diameter ($D_{average}$) over the mesopore, using the desorption branch of the isotherm.

Surface concentration of sulfonate is calculated from samples ion exchange capacity measured by acid–base titration (Tominaga et al. 2007). Firstly, synthesis samples (0.05 g) are immersed in NaCl solution (2 mol/L) and are stirred 15 h for ion exchange, and then titrates the mixed solution with NaOH standard solution (0.01 mol/L) of the exchanged H^+ amount. Finally, the samples ion exchange capacity is calculated.

2.3 Water vapor sorption

The adsorption/desorption kinetics and isotherms of the water vapor on the sulfonic modified mesoporous silica are measured on a dynamic vapor sorption system (Surface Measurement Systems Advantage 1, DVSA-STD 10052s-01). DVS advantage system is shown in Fig. 1.

Before the measurement of vapor adsorption, the samples are dried at 473 K for 2 h. Nitrogen is used as the dry carrier gas for DVS. The concentration of vapor was precisely controlled with mass flow controller and real time vapor concentration monitor. The sample weight change during water sorption/desorption can be measured by an ultra-microbalance module. When the mass change is less than 0.002 mass%/min, the samples are considered to reach the kinetic equilibrium. Based on the equilibrium moisture content at different RH, water vapor isotherms can be plotted.

The adsorption isotherms are plotted based on the equilibrium adsorption capacity at various RHs from 0 to

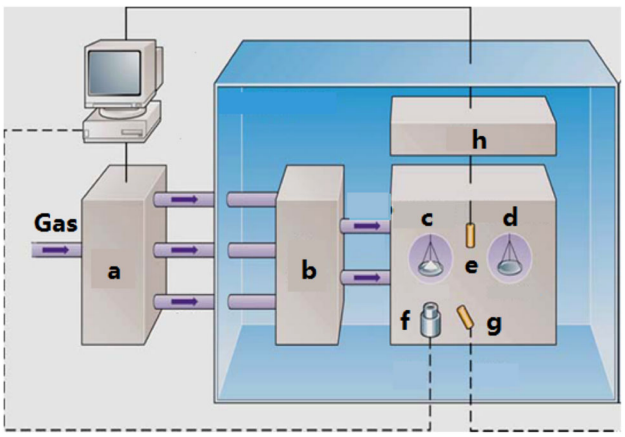

Fig. 1 DVS advantage system: *a* mass flow controller; *b* vapor generator; *c* sample; *d* reference; *e* humidity sensor; *f* camera; *g* thermometer; *h* microbalance module

90 %. The desorption kinetics are obtained by measuring the weight change of the samples with time at 360 K.

3 Computational methods

3.1 Mesoporous silica model

The first step to reproduce the sulfonic modified mesoporous silica is to build a realistic model that can represent the mesoporous silica. Then, on the basis of that model, it is possible to attach sulfonate grafts to the surface hydroxyl groups (OH) to obtain the sulfonic modified mesoporous silica, as shown in Fig. 2.

The MCM-41 pore model is generated following a procedure similar to that proposed by Coasne et al. (2006) to prepare MCM-41 model. To create bulk amorphous silica, we replicate a high-crystoballite unit cell 8 × 8 × 4, yielding a system of 6,144 atoms. This step is followed by an annealing cycle proposed by Huff et al. (1999) that employs the Morse-style potential developed by Demiralp et al. (1999). Interaction energy expression is shown in Eq. (1) and parameters are listed in Table 1.

$$U_{ij} = \frac{q_i q_j}{r} + D_0 \left\{ \exp\left[\gamma\left(1 - \frac{r}{R_0}\right)\right] - 2\exp\left[\frac{1}{2}\gamma\left(1 - \frac{r}{R_0}\right)\right]\right\} \quad (1)$$

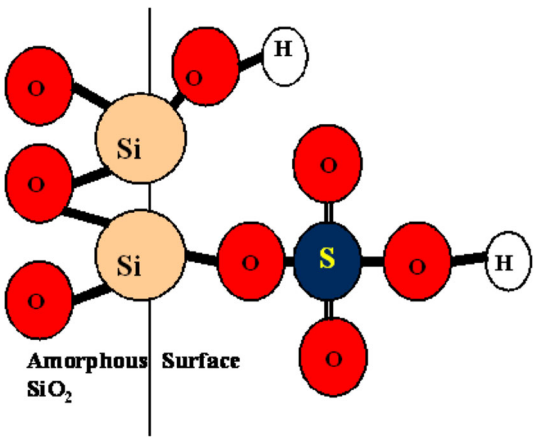

Fig. 2 Sulfonic modified mesoporous silica structure

Table 1 Morse potential parameters

Interaction	R_0 (nm)	D_0 (kcal/mol)	γ
O–O	0.3791	0.5363	10.4112
Si–Si	0.37598	0.17733	15.3744
Si–O	0.1628	45.997	8.6342

D_0 is bond strength. R_0 is bond length. γ is dimensionless force constant. r is the distance between the particles. q_i, q_j is the particle charge.

Annealing cycle is performed by Forcite package (Material Studio) in the NVT ensemble. Temperature increases from 300 to 7,000 K at a rate of 4 K/ps and then melting samples are quenched to room temperature. Amorphous sample is equilibrated for 40 ps in the NPT ensemble at a pressure of 1 bar. Bulk amorphous silica model obtained gets a lattice 5.70 × 5.70 × 2.85 nm^3 and a density of 2.205 g/cm^3. After carving out a cylindrical pore with a diameter of 4.1 nm, the structure with dangling silicon and oxygen atoms are saturated with hydroxyl group or hydrogen. Remove silicon atoms which bonded to more than two hydroxyl groups and then relax the structure by 200 ps NVT dynamics simulation.

Sulfonic modified mesoporous silica is obtained by attaching sulfonate grafts to the surface hydroxyl groups randomly (Builes et al. 2012). Different amount sulfonate grafts are attached to obtain modified samples with different surface sulfonate densities. After tether organic groups to the oxygen atom which bonded to the silica surface, the structure atoms, apart from hydroxyl groups, oxygen atoms bonded with organic groups and organic groups, are fixed and run a dynamics simulation in NVT ensemble for relaxation with CVFF forcefield.

Structure characterization is performed by Atom Volume & Surface module in Material Studio. Accessible surface areas can be used to evaluate the BET surface with a solvent radius of 0.184 nm (Düren et al. 2007). The accessible surface areas are calculated by rolling a probe molecule over the framework surface. Surface sulfonate density is shown in $mmol/m^2$ by dividing the S_{BET} for convenient comparison.

3.2 Simulation methodology

We perform grand canonical Monte Carlo (GCMC) simulations to compute the adsorption of both nitrogen molecules in pristine structure and water vapor in surface modified structure. The GCMC method is a stochastic process that simulates sorbent in equilibrium with an infinite reservoir of fluid at fixed chemical potential and temperature. The absolute adsorption isotherm is evaluated by the ensemble average of the number adsorbed atoms as a function of the pressure of the fluid reservoir (pressure of the reservoir is obtained from the chemical potential, according to the bulk equation of state for an ideal fluid). Periodic boundary conditions are applied in all the three dimensions. Interactions between adsorbate and adsorbent are calculated by the sum of a Lennard–Jones 12–6 potential and a Coulombic electrostatic contribution.

Interaction energy expression is shown as Eq. (2). The cross interaction parameters between different atoms are calculated using Lorentz-Berthelot combination rules, as shown in Eq. (3). Where ε_{ij} is depth of the potential well. σ_{ij} is the finite distance at which the inter particle potential is zero. r_{ij} is the distance between particles and ε_0 is the electric constant, which has the value of 8.854,187,817 $\times$ 10^{-12} Fm^{-1}.

$$U_{ij}(r) = 4\varepsilon_{ij}\left[\left(\frac{\varepsilon_{ij}}{r_{ij}}\right)^{12} - \left(\frac{\varepsilon_{ij}}{r_{ij}}\right)^{6}\right] + \frac{q_i q_j}{4\pi\varepsilon_0} \quad (2)$$

$$\begin{cases} \sigma_{ij} = \frac{\sigma_{ii}+\sigma_{jj}}{2} \\ \varepsilon_{ij} = \sqrt{\varepsilon_{ii}\varepsilon_{jj}} \end{cases} \quad (3)$$

For nitrogen sorption simulation, a spherical Lennard–Jones model is used for nitrogen and parameters are list in Table 2 (Maddox and Gubbins 1995). For time saving, nitrogen atoms are only operated by insertion and deletion. For each value of pressure below $0.4P_0$, 1.0 $\times$ 10^7 trials are used for equilibration and production. Simulations at other pressure values use 2.0 $\times$ 10^7 trials.

Water sorption simulation is performed to study water sorption mechanism in surface modified sorbent in low RH. TIP3P model is used during the water sorption simulation (Jorgensen et al. 1983). Operations on water atoms during the simulation are Exchange, Rotate, Translate, and Regrowth with a ratio of 2:1:1:0.1. Each simulation involves 2.0 $\times$ 10^7 trials for equilibration and another 2.0 $\times$ 10^7 trials for production. Forcefield parameters of the modified sorbent for GCMC simulation are provided in the supporting materials.

4 Results and discussion

4.1 Material characterization

The nitrogen adsorption–desorption isotherms of four sulfonic acid-modified mesoporous silica are shown in Fig. 3. The adsorption isotherms belong to type IV isotherms, with the characteristic of multi-layer adsorption accompanied with capillary condensation. Shapes of the hysteresis loop indicate the cylindrical pore structure of the sorbents (De Boer et al. 1958). Pore size distribution analyzed by BJH model is shown in Fig. 4. Compared with S–SiO_2–B, S–SiO_2–C and S–SiO_2–D, S–SiO_2–A has a narrower pore size distribution, representing the uniform pore size, which was chosen to be the prototype for molecular simulation. Textural properties of the sulfonic acid-modified mesoporous silica samples and a reference sample of MCM-41 are listed in Table 3.

Table 2 Parameters for nitrogen sorption simulation at 77 K

Atom types	σ (nm)	ε (K)
bO	0.278	185
N	0.375	190
nbO	0.3	190

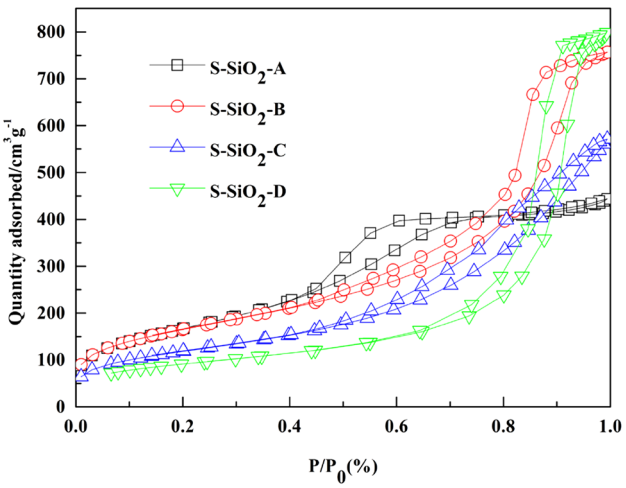

Fig. 3 Nitrogen adsorption–desorption isotherm

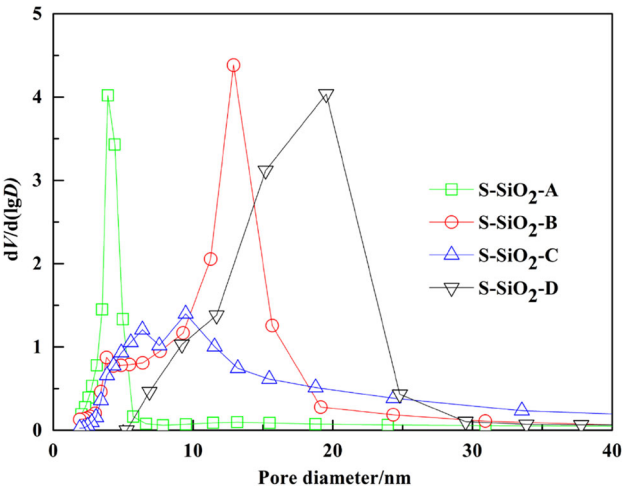

Fig. 4 BJH pore size distribution curves

4.2 Water sorption over the sulfonic acid-modified mesoporous silica

Generally, the mechanism of water vapor adsorption follows: (1) the adsorption of water on surface functional groups; (2) the adsorption of water on previously adsorbed water molecules and subsequent cluster formation; (3) pore filling occurs at condensation pressure; (4) a plateau is reached at high pressure when all pore are filled (Brennan et al. 2001). Water vapor adsorption isotherms of four mesoporous sorbents are shown in Fig. 5, compared with a

Table 3 Textural properties of the sulfonic acid-modified mesoporous silica samples

Name	S_{BET} (m^2/g)	V_{pore} (cm^3/g)	$D_{average}$ (nm)	Q[a] (mg/g)
S–SiO_2–A	607	0.73	4.16	693.0
S–SiO_2–B	586	1.14	8.1	546.7
S–SiO_2–C	420	0.88	8.0	470.3
S–SiO_2–D	326	1.34	13.1	334.5

[a] Water vapor sorption capacity at 90 % RH

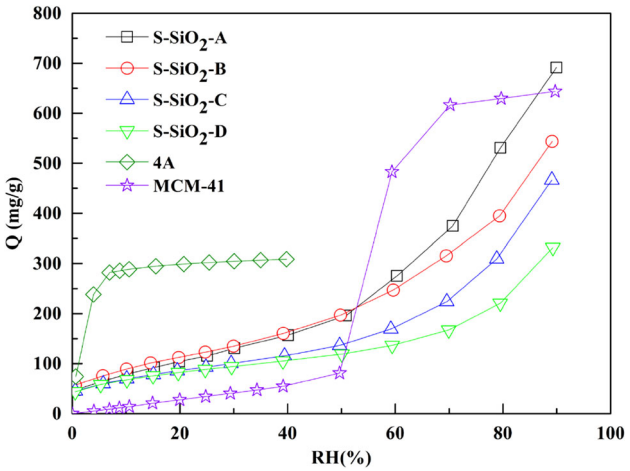

Fig. 5 Adsorption isotherms of water over the sulfonic acid-modified mesoporous silica samples at 298 K

mesoporous MCM-41 and a micro porous 4A zeolite. All the mesoporous isotherms show capillary condensation due to the mesopore distributions. At low RH (<50 %), water sorption capacity follows the order of 4A zeolite > sulfonic acid-modified mesoporous silica samples >MCM-41. The highest sorption capacity of 4A zeolite can be attributed to its strong affinity of micropores to water. The higher water adsorption capacity of sulfonic acid-modified mesoporous silica samples than MCM-41 is due to the presence of stronger hydrophilic sites, –SO_3H functional groups over the sulfonic acid-modified mesoporous silica samples, which promote the cluster formation of adsorbed water molecules. The results further confirm that the introduction of –SO_3H functional groups to mesoporous silica samples during synthesis. For MCM-41, hydroxyl groups on the pore surface could act as the adsorption sites for water molecules via weak H-bonding interaction. The sorption capacities of four sulfonic acid-modified mesoporous silica samples are quite close at low relative humidity, suggesting the amounts of –SO_3H functional groups introduced are similar. At higher RH (>50 %), the sorption capacity of four sulfonic acid-modified mesoporous silica samples follows the order of S–SiO_2–A > S–SiO_2–B > S–SiO_2–C > S–SiO_2–D, which is consistent with the order of BET surface area.

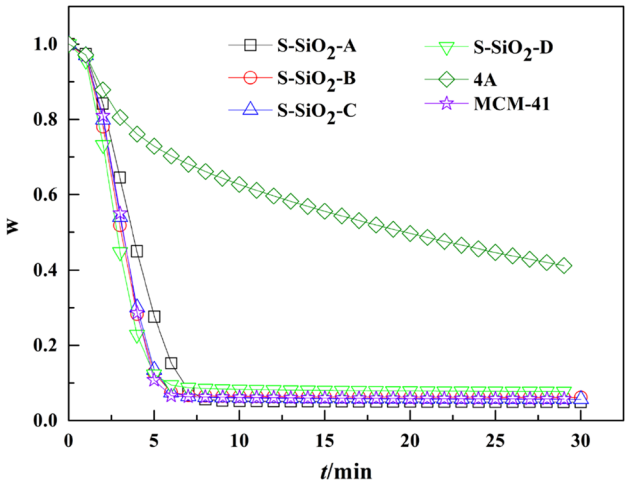

Fig. 6 Desorption curves of water vapor over the sulfonic acid-modified mesoporous silica samples at 360 K

4.3 Water desorption over the sulfonic acid-modified mesoporous silica

For the practical application, i.e., rotary desiccant dehumidifier, the sorbents should possess not only high dehumidification capacity but also fast desorption kinetics for high energy efficiency. Figure 6 shows the desorption curves of water vapor over the sulfonic acid-modified mesoporous silica samples at 360 K. Desorbed water contents after 30 min are listed in Table 4. The desorption kinetics follow the order of sulfonic acid-modified mesoporous silica > MCM-41 > 4A zeolite. Compared to zeolite 4A possessing high water sorption capacity at low RH, sulfonic acid-modified mesoporous silica samples as well as MCM-41 show a faster desorption rate and the desorbed water contents reached above 90 % after 10 min. The above results suggest that sulfonic acid-modified mesoporous silica has relative high water sorption capacity and fast desorption kinetics.

4.4 Molecular simulation

Water adsorption over the sulfonic acid-modified mesoporous silica samples was studied computationally. Before GCMC simulation, we need to prepare an accurate sorbent structure. For bulk amorphous silica structure, the density and radial density functions of Si, O were calculated as shown in Table 5, which were close to the experiment results (Bourg and Steefel 2012), suggesting the modeled amorphous structure has similar atom array with the experiment samples. Moreover, the density of –OH obtained (6.25 OH/nm^2) is close to that obtained experimentally for porous silica (5–7 OH/nm^2) (Landmesser et al. 1997).

Table 4 Desorption water contents in 30 min at 360 K

Name	Desorbed water amount (%)
S–SiO_2–A	96.94
S–SiO_2–B	93.86
S–SiO_2–C	94.32
S–SiO_2–D	92.25
4A zeolite	58.8
MCM-41	94.3

Table 5 Bulk amorphous silica properties

	Experiment	Simulation
Si–O (1st) (nm)	0.16	0.165
Si–O (2nd) (nm)	0.413	0.415
Si–Si (1st) (nm)	0.31	0.32
O–O (nm)	0.261	0.265
Bulk density (cm^3/g)	2.20	2.205

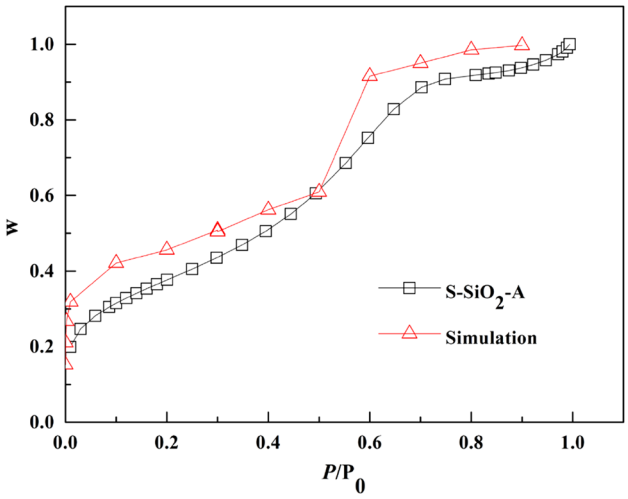

Fig. 7 Comparison of nitrogen sorption isotherms of simulated silica model, S–SiO_2–A and MCM-41 at 77 K

Simulation results of nitrogen sorption isotherm of the constructed mesoporous silica are compared to that of S–SiO_2–A from the experimental results as shown in Fig. 7. Both have a similar shape of isotherm. The capillary condensation occurs at similar pressure range for S–SiO_2–A and the constructed silica model, which indicates that the constructed model has similar pore size as the synthesized S–SiO_2–A. The consistency suggests the constructed silica model can represent the synthesized S–SiO_2–A from experiment.

Silica with different surface sulfonate densities were modeled with the textural properties with the characterization parameters as shown in Table 6. Both surface area and pore volume decrease by increasing grafted –SO_3H functional groups on silica surface. Modeled structures have much lower surface area than experiment sample, which is because the pore structures in the modeled structure are constructed with uniform mesopores while the synthesized samples have a combination of micropore and mesopore. Regardless of surface area, the synthesized structure can be well represented by the modeled silica structure with close pore size and similar functional surface group density.

Simulation results of water sorption are compared with that of S–SiO_2–A experimentally at low RH. Simulation result of 30S–SiO_2 is compared with S–SiO_2–A in Fig. 8 due to the similar sulfonate density. Simulated water sorption over 30S–SiO_2 at different RH of 5, 10, 15, 20, 30, 40 % were simulated and showed good consistency with experimental results, which suggests the validation of simulation method and forcefield parameters for the simulated –SO_3H modified mesoporous silica model. A micro-view of water molecule adsorption over –SO_3H modified mesoporous silica from simulation showed in Fig. 9, adsorbed water molecules are noted to accumulate around hydrophilic –SO_3H groups and form water molecule clusters via hydrogen bond.

Water vapor sorption isotherms of modeled silica grafted with different sulfonate densities are simulated as shown in Fig. 10. Radius density distribution of adsorbed water molecule is presented in Fig. 11. Q_S is the sorption capacity per surface area. Peak density of water sorption over mesoporous silica appears around 20 angstrom, close to the radius of pore, suggesting water molecules were adsorbed on silica surface predominantly. By introducing higher surface sulfonate density, peak density around the pore surface becomes larger, while the density inside the pores of silica is almost unchanged. Peak density around surface increases with RH. Water density increases toward the pore center, which may be the sign of transformation from surface adsorption to water vapor condensation. Radius density distribution shows that water molecules are adsorbed around the pore surface first, and then turn to condensation to fill the pore. It is obvious that the sorption capacity increases with surface sulfonate density on silica. But it is uncertain to ascribe this increase of sorption capacity merely to the water-hydrophilic group interaction, which can be complemented by elucidating the sorbate-sorbent interaction. Therefore, the H_2O^- –SO_3H grafted silica interaction is further studied computationally.

Intermolecular interaction is defined as all intermolecular interactions in the sorbate–sorbent configuration which consists of interaction between sorbate molecules and between sorbate and sorbent framework. It can be used to evaluate the development of adsorption mechanism via its

Table 6 Characterization of different simulation structures

Name	S_{BET} (m^2/g)	V_{pore} (cm^3/g)	Sulfonate density ($\times 10^{-3}$ mmol/m^{-2})
S–SiO_2–A	607	0.73	1.169
1S–SiO_2	361	0.25	0.036
20S–SiO_2	317	0.19	0.810
30S–SiO_2	362	0.22	1.051
40S–SiO_2	356	0.22	1.416
SiO_2	315	0.20	\

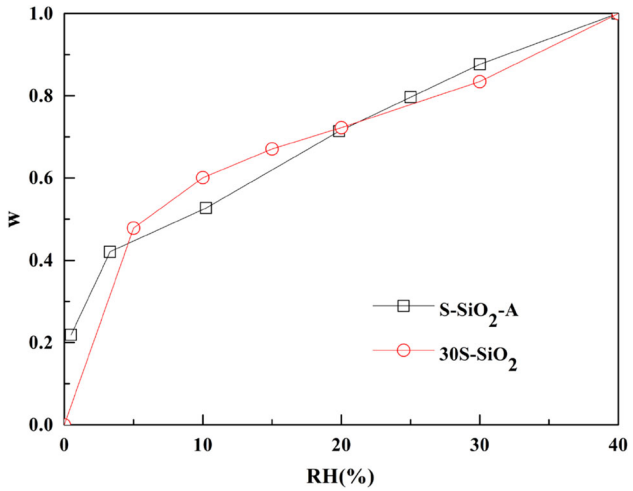

Fig. 8 water vapor sorption isotherms at 298 K

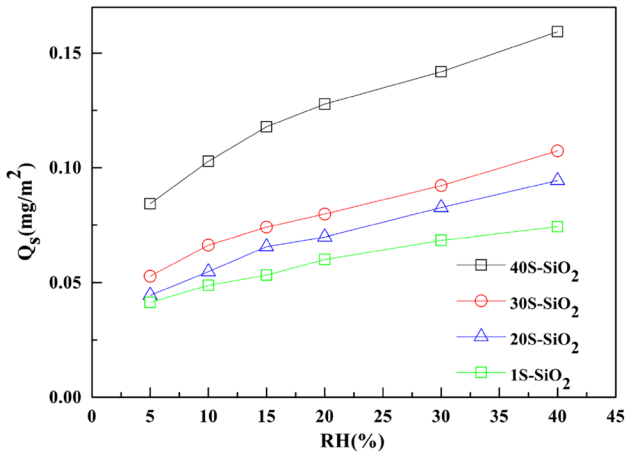

Fig. 10 Water vapor sorption isotherms of simulated structures with different sulfonate densities at 298 K

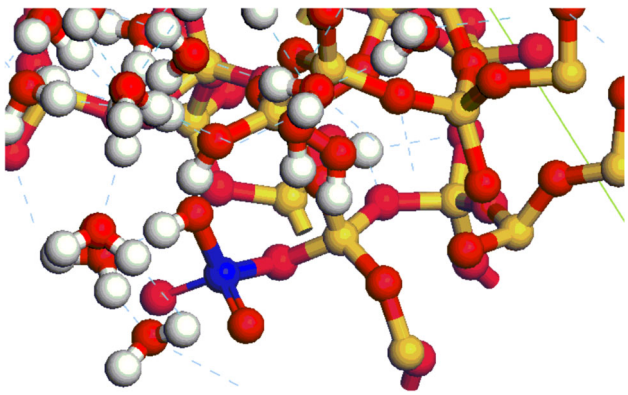

Fig. 9 Micro-view of water sorption around sulfonic groups in simulation (*white ball* hydrogen; *red ball* oxygen; *blue ball* sulfur; *yellow ball* silicon; *Dashed line* hydrogen bond symbol) (Color figure online)

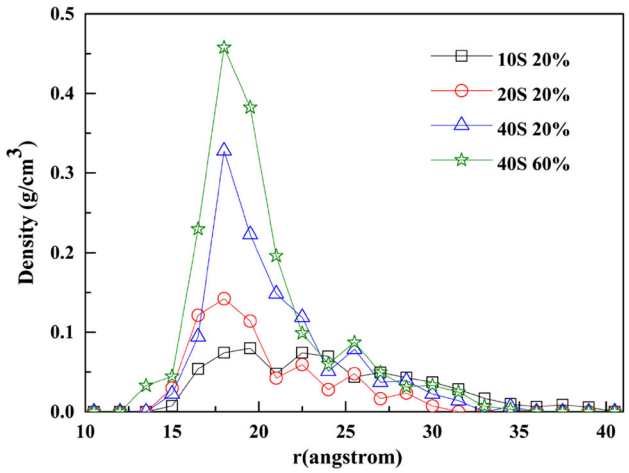

Fig. 11 Radius density distribution of adsorbed water molecule

transformation. Intermolecular interactions of different samples are calculated at RH of 20 % and the distribution probability is shown in Fig. 12. Compare to 1S–SiO_2, intermolecular interaction of SiO_2 is centralized around −10 to −20 kcal/mol while that of 1S–SiO_2 are distributed in two regions (weak interaction of −20 to −10 kcal/mol, strong interaction of −40 to −20 kcal/mol). Centralized energy distribution of intermolecular interaction of SiO_2 indicates H_2O–SiO_2 is dominated by one type of interaction. For SiO_2, surface –OH groups can form H-bond with water molecules, which have similar binding energy with that of the water–water intermolecular H-bonding. Higher intermolecular interaction of 1S–SiO_2 corresponds to strong interaction between water molecules and sulfonate groups. As the sorption capacity of 1S–SiO_2 is small, the difference in the proportions of water adsorbed by sulfonate groups, OH groups and water–water cluster

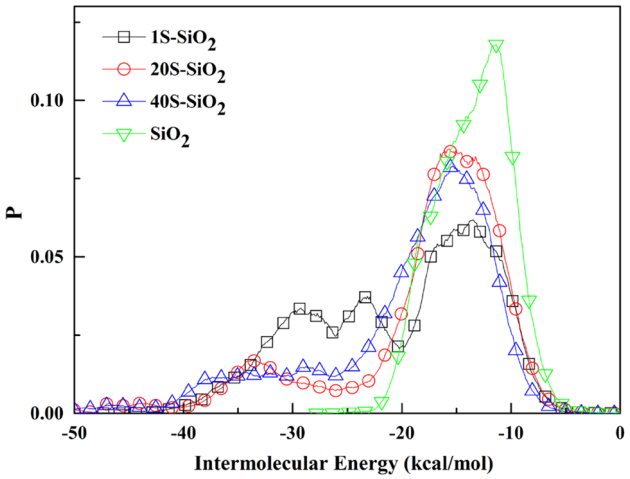

Fig. 12 Energy distribution of intermolecular interaction at 20 % RH

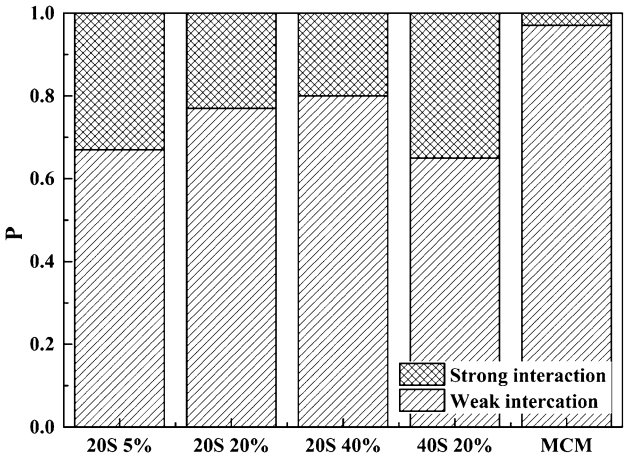

Fig. 13 Probability of strong and weak interaction adsorbed proportion

formation is not significant. Compared 20S–SiO_2 and 40S–SiO_2 with 1S–SiO_2, the difference in energy distribution of intermolecular interaction between strong interaction area and weak interaction region increases as the probability of weak interaction area increases with surface sulfonate density. This indicates that surface hydrophilic groups could promote the water–water intermolecular H-bonding process and thus more water molecules adsorbed via weak interaction. The result confirms that the increase in sorption capacity with surface sulfonate density is not merely a result of strong interaction between hydrophilic –SO_3H groups and water molecules. Integral probability of weak and strong interaction adsorbed proportion are compared in Fig. 13. Weak interaction adsorbed proportion increases with RH and decreases in surface sulfonate density.

From the simulation snapshot as shown in Fig. 14, there are more water molecules in cluster than accumulation around sulfonate groups. Combine with the above analysis, water molecules are adsorbed around sulfonate groups through strong interaction. Then more water molecules will be adsorbed by the weak H_2O–H_2O intermolecular H-bonding interaction to form H_2O clusters. Surface sulfonate sites act as the adsorption center for water molecules, but the dominate proportion of adsorbed water molecules is bonded through weak intermolecular H-bonding interaction.

5 Conclusion

Experimental and numerical studies concerning H_2O adsorption over –SO_3H modified mesoporous silica are carried out. The following conclusions can be drawn:

(a) Experimental results show that mesoporous silica functionalized by sulfonate have higher water sorption capacity and fast desorption kinetics.
(b) Higher density of –SO_3H group led to higher water sorption capacity due to a strong sulfonate–water interaction based on the validated –SO_3H modified mesoporous silica model.

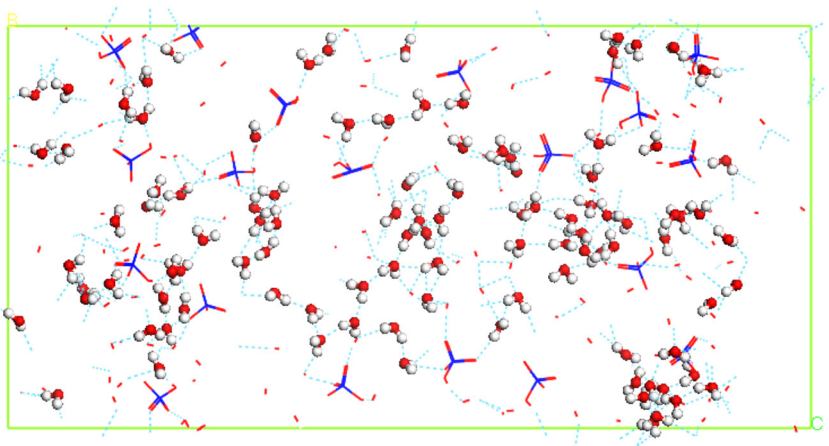

Fig. 14 Snapshot of simulation of 40S 20 % (*blue* site mean sulfonate groups; *white* and *red balls* are water molecules; *dashed line* is the hydrogen bond system) (Color figure online)

(c) Combined simulation results of energy distribution of intermolecular interaction and micro-view of water sorption over $-SO_3H$ modified silica reveal the presence of two types of adsorption. Although strong interaction (intermolecular interaction of -40 to -20 kcal/mol) between hydrophilic–SO_3H with water can increase water sorption capacity of sorbent at low RH, weak H_2O–H_2O interaction (intermolecular interaction of -20 to -10 kcal/mol) dominated water sorption capacity at both low and high RH. Further study elucidating water sorption mechanism over sulfonate-grafted silica should be carried on to guide the specific desiccant design.

Acknowledgments We are pleased to acknowledge the funding support by NSFC-Guangdong Joint Fund Project (U1034005), National Natural Science Foundation of China (51106185), Nature Science Foundation of Guangdong Province (S2012040007694), Fundamental Research Funds for the Central Universities (121gpy23) and National Basic Research Program of China (2012CB720404).

References

Bourg, I.C., Steefel, C.I.: Molecular dynamics simulations of water structure and diffusion in silica nanopores. J. Phys. Chem. C **116**(21), 11556–11564 (2012)

Brennan, J.K., Bandosz, T.J., Thomson, K.T., Gubbins, K.E.: Water in porous carbons. Colloids Surf. A **187**, 539–568 (2001)

Builes, S., Lopez-Aranguren, P., Fraile, J., Vega, L.F., Domingo, C.: Alkylsilane-functionalized microporous and mesoporous materials: molecular simulation and experimental analysis of gas adsorption. J. Phys. Chem. C **116**(18), 10150–10161 (2012)

Coasne, B., Galarneau, A., Di Renzo, F., Pellenq, R.J.M.: Gas adsorption in mesoporous micelle templated silicas: Mcm-41, mcm-48, and sba-15. Langmuir **22**(26), 11097–11105 (2006)

De Boer, J.H., Everett, D.H., Stone, F.S.: The Structure and Properties of Porous Materials, vol. 10, p. 68. Butterworths, London (1958)

Demiralp, E., Çağin, T., Goddard III, W.A.: Morse stretch potential charge equilibrium force field for ceramics: application to the quartz-stishovite phase transition and to silica glass. Phys. Rev. Lett. **82**(8), 1708 (1999)

Düren, T., Millange, F., Férey, G., Walton, K.S., Snurr, R.Q.: Calculating geometric surface areas as a characterization tool for metal-organic frameworks. J. Phys. Chem. C **111**(42), 15350–15356 (2007)

Ho, L.N., Perez Pellitero, J., Porcheron, F., Pellenq, R.J.M.: Enhanced co_2 solubility in hybrid mcm-41: molecular simulations and experiments. Langmuir **27**(13), 8187–8197 (2011)

Huff, N.T., Demiralp, E., Cagin, T., Goddard III, W.A.: Factors affecting molecular dynamics simulated vitreous silica structures. J. Non-Cryst. Solids **253**(1), 133–142 (1999)

Jorgensen, W.L., Chandrasekhar, J., Madura, D.J., Impey, R.W., Klein, M.L.: Comparison of simple potential functions for simulating liquid water. J. Chem. Phys. **79**(2), 926–935 (1983)

Kocherbitov, V., Alfredsson, V.: Hydration of mcm-41 studied by sorption calorimetry. J. Phys. Chem. C **111**(35), 12906–12913 (2007)

Landmesser, H., Kosslick, H., Storek, W., Fricke, R.: Interior surface hydroxyl groups in ordered mesoporous silicates. Solid State Ion. **101**, 271–277 (1997)

Li, X., Li, Z., Xia, Q., Xi, H.: Effects of pore sizes of porous silica gels on desorption activation energy of water vapour. Appl. Therm. Eng. **27**(5), 869–876 (2007)

Maddox, M.W., Gubbins, K.E.: Molecular simulation of fluid adsorption in buckytubes. Langmuir **11**(10), 3988–3996 (1995)

Mancinelli, R., Imberti, S., Soper, A.K., Liu, K.H., Mou, C.Y., Bruni, F., Ricci, M.A.: Multiscale approach to the structural study of water confined in mcm41. J. Phys. Chem. B **113**(50), 16169–16177 (2009)

Roque-Malherbe, M.M.A.: Adsorption and Diffusion in Nanoporous Materials. CRC Press, Florida (2007)

Schumacher, C., Gonzalez, J., Perez-Mendoza, M., Wright, P.A., Seaton, N.A.: Design of hybrid organic/inorganic adsorbents based on periodic mesoporous silica. Industrial Eng. Chem. Res. **45**(16), 5586–5597 (2006)

Tominaga, Y., Hong, I.-C., Asai, S., Sumita, M.: Proton conduction in nafion composite membranes filled with mesoporous silica. J. Power Sour. **171**(2), 530–534 (2007)

Wang, W.L., Wang, X.X., Song, C.S., Wei, X., Ding, J., Xiao, J.: Sulfuric acid-modified bentonite as the support of tetraethylenepentamine for CO_2 capture. Energy Fuels **27**(3), 1538–1546 (2013)

Wang, W.L., Xiao, J., Ding, J., Wang, X.X., Song, C.S.: Development of a new clay supported polyethylenimine composite for CO_2 capture. Appl. Energy **113**, 334–341 (2014)